



ELSEVIER

Applied Surface Science 202 (2002) 183–198

applied
surface science

www.elsevier.com/locate/apsusc

Surface compositional changes in GaAs subjected to argon plasma treatment

C.C. Surdu-Bob^a, J.L. Sullivan^{a,*}, S.O. Saied^a, R. Layberry^a, M. Aflori^b

^aSurface Science Group, School of Engineering and Applied Science, Aston University, Birmingham B47ET, UK

^bPlasma Physics Department, A.I.I. Cuza University, Iasi 6600, Romania

Abstract

X-ray photoelectron spectroscopy (XPS) has been employed to study surface compositional changes in GaAs (1 0 0) subjected to argon plasma treatment. The experimental results have been explained in terms of predicted argon ion energies, measured ion densities and etch rates. A model is proposed for the processes taking place at the surface of GaAs in terms of segregation, sputtering and surface relaxation. Stopping and range of ions in matter (SRIM) code [1] has also been employed as an aid to identification of the mechanisms responsible for the compositional changes. Argon plasma treatment induced surface oxidation at very low energies and sputtering and surface damage with increasing energy.

© 2002 Published by Elsevier Science B.V.

PACS: 81.05.Ea

Keywords: GaAs; Argon plasma; Etching

1. Introduction

Reactive ion etching is widely used in the fabrication of III–V semiconductor devices. This method involves a combination of physical and chemical interactions with the surface of semiconductor. For a complete understanding of the phenomena taking place when the semiconductor is exposed to energetic reactive ions, a separation of the physics and chemistry is necessary. In this study, we have used GaAs (1 0 0) surfaces exposed to argon plasmas over a range of pressures and RF powers to help achieve this aim.

To our knowledge, very little work on etching of GaAs with argon RF plasmas has been reported [2],

although monoenergetic argon ion bombardment of GaAs has been studied extensively in the energy range of 20–100 keV [3] and at lower energies of a few keV [4–11]. Diagnosis of RF argon plasma has also been reported [12–14]. When etching with inert gases not only physical bombardment processes, but surface oxidation processes occur. The results strongly suggest that H₂O present in the process chamber, residual oxygen and oxygen from the reduced native oxides of the sample surface are the main sources for oxygen involved in surface oxidation.

2. Experiment

The plasma etcher used was an asymmetrical capacitively-coupled industrial Oxford Instruments Plasma

* Corresponding author. Tel.: +44-121-3590156x5276.
E-mail address: j.l.sullivan@aston.ac.uk (J.L. Sullivan).

Technology System 100 powered at 13.56 MHz and controlled from a PC. A quartz plate, of thickness 12 mm, covered the powered electrode. The ranges of experimental etching pressure and power were 1×10^{-2} to 12×10^{-2} mbar and 5–200 W, respectively. The background pressure was always better than 10^{-6} mbar and the Ar flow rate was 14.1 cm^3 .

A Hiden Analytical Langmuir probe, attached to the plasma cell, was used to determine plasma potential and ion density. The dc bias and the driving potential at the cathode were also measured.

X-ray photoelectron spectroscopy (XPS) analysis for this work was carried out in an VGS ESCALAB 200D spectrometer using Al K α unmonochromatized radiation (1486.6 eV, FWHM = 0.8 eV) at an anode voltage of 15 kV. The analyser pass energy was 20 eV and the energy step size was 0.05 eV. The spectra were acquired and processed using Eclipse software installed in the instrument data system. For the fitting procedure performed on Ga 3d and As 3d peaks, 30% Gaussian and 70% Lorentzian line shapes were used. Corrections of the charge shift was accomplished by taking As (GaAs) at 41.1 eV as [15]. Sensitivity factors for the Ga and As lines were previously determined in our laboratory [6]. Angle resolved XPS (ARXPS) was performed at take-off angles between 0 and 70° relative to the normal of the sample surface, corresponding to analysis depths of 67 and 23 Å, respectively [11]. The calculation of oxide thickness was based on the model described by Briggs and Seah [16] and an electronic mean free path value of 26 Å was used [11]. For topography changes and determination of etch pit depths, a topometrix explorer atomic force microscope (AFM) was employed.

The GaAs samples were polished wafers cleaned for 15 min in acetone and a further 15 min in isopropanol using an ultrasonic bath. For determination of etch rates, a small piece of GaAs was placed on top of a larger piece of the same material and the whole was etched in the plasma. Thus, the area under the small sample was not subjected to the plasma. The small sample was removed and the etch depth was measured by measuring the step size using line scans from AFM traces. The time of exposure to plasma was 30 min for all samples.

Water adsorbed on the chamber walls of the plasma etcher is an important contaminant. At base pressures as low as of 10^{-9} mbar surface water is the major cell

contaminant and can consist of over 100 monolayers. During plasma processing, ions bombard the chamber walls and remove H₂O which then suffers dissociation in the active plasma. Thus, the water adsorbed on the chamber walls becomes source of oxygen and hydrogen species in the plasma.

A rough estimation of the partial pressure of impurity oxygen originating from dissociation of water can be easily obtained. The ionization coefficient of low temperature plasmas is 10^{-3} . Suppose that the concentration of active species of oxygen (oxygen ions, ozone ions etc.) has a maximum value of 1%. For a vacuum of 10^{-6} mbar (used in this work), the partial pressure of active oxygen present as impurity is $10^{-3} \times 10^{-6}$ mbar. Argon plasma is efficient for desorption of H₂O from the walls, hence for a similar background pressure, a higher amount of oxygen species is expected to appear in this plasma compared to plasmas of other gases.

Another important source of oxygen impurities in the plasma is the feed gas. The argon gas used in this work had high purity (99.999%) standard industrial grade and the impurities did not exceed: 4 ppm O₂, 15 ppm N₂ and 1 ppm H₂. The partial pressure of oxygen at the extreme values used in this work, 1×10^{-2} and 12×10^{-2} mbar is $4 \times 10^{-4} \times 1 \times 10^{-2}$ and $4 \times 10^{-4} \times 12 \times 10^{-2}$ mbar, respectively. The partial pressure of active oxygen introduced by 4 ppm O₂ at these pressures is $4 \times 10^{-4} \times 10^{-3}$ and $36 \times 10^{-4} \times 10^{-1}$ mbar, respectively. These values show that the partial pressure of impurity oxygen contained in the feed gas is even more important than that introduced by adsorbed water on the process chamber walls.

Thus, sample to sample variations were caused by variation in the cell condition and this is evident in any commercial plasma cell. Variation of plasma composition with power and pressure in an industrial RF plasma is presented by Russu [22].

XPS analysis introduced errors due to both spectrum acquisition and spectrum processing. Poor statistics of spectrum acquisition is an important factor. A significant source of errors is due to accuracy of spectrum fitting, also. These errors were minimized by using rigorously the same procedure for spectrum fitting. According to our evaluation, in this work, this procedure did not introduce an error greater than 10%.

The experimental error consists of the sum of the errors caused by plasma processing and XPS instrument (XPS data acquisition and processing). The errors due to plasma processing are difficult to evaluate. However, care was taken to ensure that the cell condition was similar for all experiments.

3. Results

3.1. Plasma characterization—ion density and energy

To understand the processes taking place when the surface is exposed to plasma, both energy and densities of plasma constituents need to be known. A change in plasma input parameters (gas pressure, RF power) causes a change in the number and velocity at the surface of active species generated. There are two major collisional processes between argon ions and neutrals which can affect both parameters, these are charge exchange and elastic collisions which have comparable cross-sections.

The RF field gives energy to the electrons, whereas the ions gain energy during acceleration across the plasma sheath under the influence of the dc bias at the cathode. At low pressures ($<10^{-1}$ mbar), the ions cross the sheath without colliding. Their mean energy can be directly determined from the potential difference between the plasma and the cathode. For pressures used in this work (over 10^{-2} mbar) this approach would not give accurate ion energies due to collisions within the sheath which scatter ions and lower their energies. In this case, one must take into account the cross-sections of the processes by modelling. In order to determine ion energies and fluxes at the cathode, a model has been developed in our laboratory which follows electrons and ions through time varying potentials [17]. The variation of ion energy distribution (IED) with power and pressure given by this code is shown in Fig. 1(a) and (b), respectively. The peaks observed in these energy distributions are due to differences in phase at which an ion enters the sheath. Also, sheath width changes with pressure induce formation of peak structures in the energy distributions. Therefore, the highest double peak is observed at 2.6×10^{-2} mbar. At high pressure all such peaks disappear and a continuum is obtained. As expected, at

higher powers the number of ions having higher energies increased whereas with increasing pressure, it decreased.

Surface changes are also dependent on flux of ions incident on the cathode surface, which is in turn dependent on the plasma ion density. This was measured using the Langmuir probe and is shown as a function of pressure in Fig. 2. The current density was calculated using the Child–Langmuir law from measured sheath width for each condition, the ion mass, the ion charge, the electronic mean free path and the measured dc bias [13]. The current density of ions is shown, as a function of pressure for different powers, in Fig. 3.

3.2. Surface changes

Exposure of GaAs to the argon plasma results mainly in physical etching with etch rate directly dependent on ion energy and ion flux. However, chemical processes (that is oxidation) also take place, as will be detailed later in this section.

3.2.1. AFM investigation

Using AFM, etch depths were determined. In Fig. 4, variation of etch depth with pressure for different RF powers for argon plasma is presented. Etch rates were calculated from the mean depth of the pit for each plasma condition. The experimental sputtering yield Y can then easily be evaluated using the following:

$$Y = \frac{er \times N_{\text{GaAs}}}{\phi}$$

where $N_{\text{GaAs}} = 5 \times 10^{22}$ atoms/cm³, er the measured etch rate and ϕ the ion flux density. The variation of the experimental yield with pressure for different powers is given in Fig. 5. The yield increased with power and decreased with pressure. This shows that the sputter yield increases with ion energy, as found by other workers [18], and decreases with pressure. Theoretical calculation of Y using stopping and range of ions in matter (SRIM) code is presented in Section 3.

3.2.2. XPS investigation

A typical synthesized spectra of a clean GaAs wafer is shown in Fig. 6. XPS analysis of this sample revealed equal quantities of Ga and As oxides, with

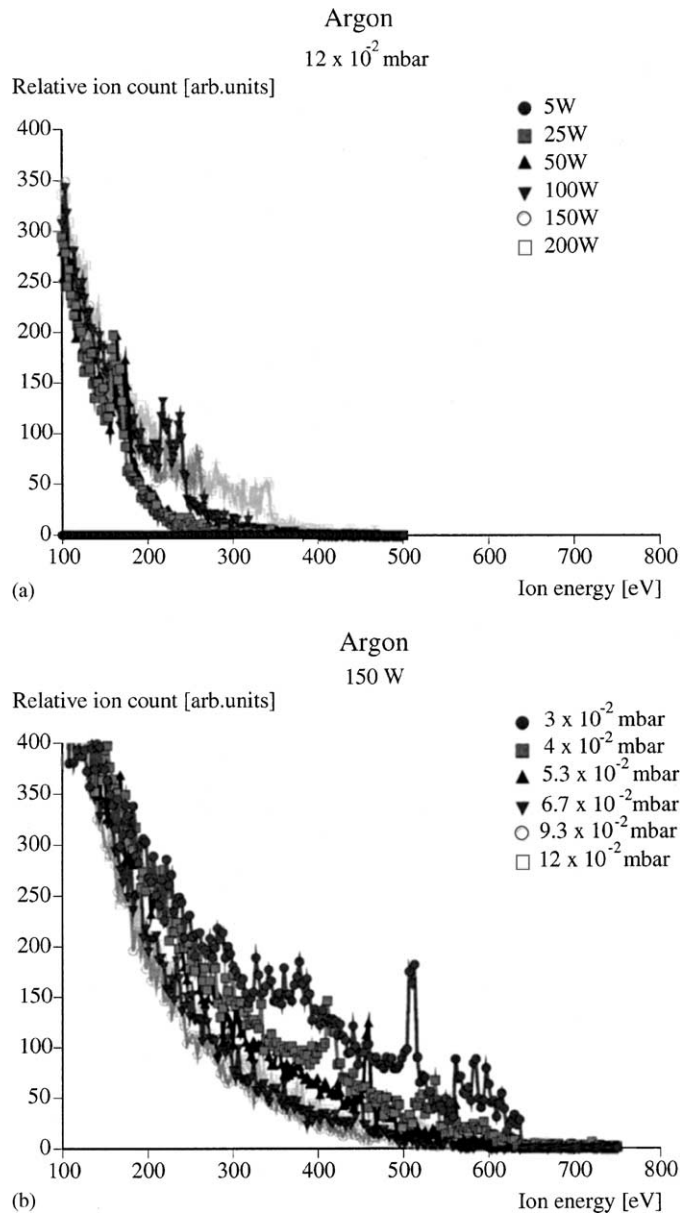


Fig. 1. Variation of ion energy distribution (IED) with power (a) and with pressure (b).

a total oxide thickness of 0.9 nm [15]. Mechanical polishing of the surface did not change this situation. This 1:1 ratio of Ga and As oxides was impossible to reproduce in our experiments using plasma or wet chemical etching.

An important experiment in our work was the study of surface compositional changes with elapsed time

after plasma treatment (Fig. 7(a)). The data showed that immediate sub-surface relaxation continues after plasma treatment. Surface oxidation in air has also taken place and exhibited a logarithmic increase with time. The oxide thickness increased by about five monolayers over a period of 13 months after plasma treatment (Fig. 7(b)).

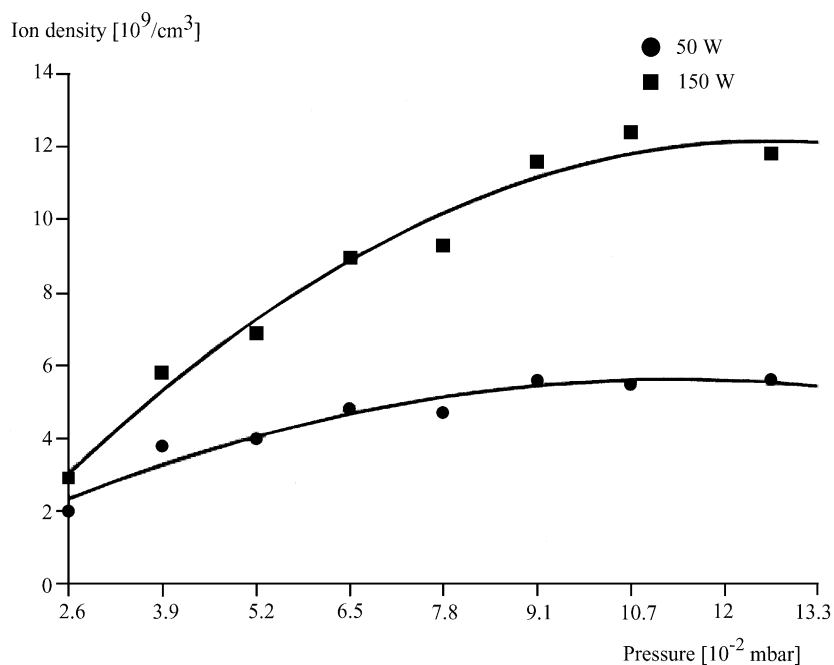


Fig. 2. Variation of ion density with pressure.

All our XPS data were acquired after about 1 month from the plasma treatment. Variation of surface composition for all pressure—power combinations is illustrated in two sets of graphs; variation of pressure at two different powers (50 and 150 W) and

variation of power at two different pressures (1 and 12 mbar), Fig. 8(a–d), respectively. The only oxide whose concentration increased with increasing pressure at 50 W was Ga_2O_3 . The main difference in the variation with pressure at 50 and 150 W was in the

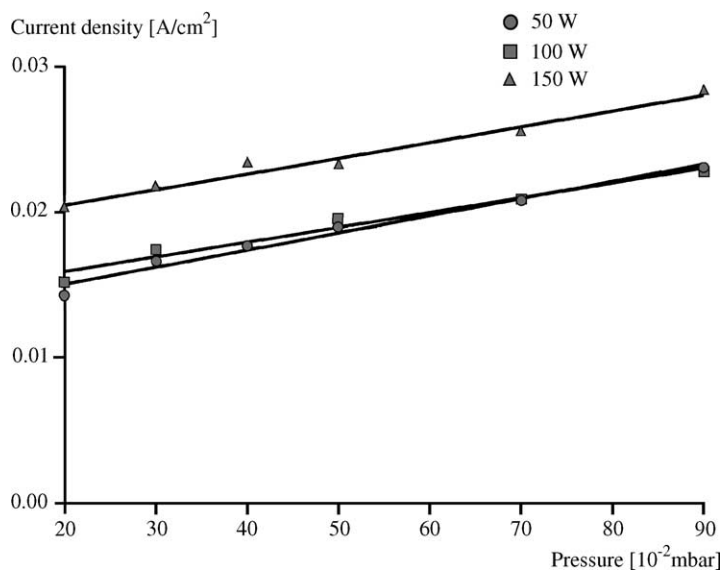


Fig. 3. Variation of current density with pressure.

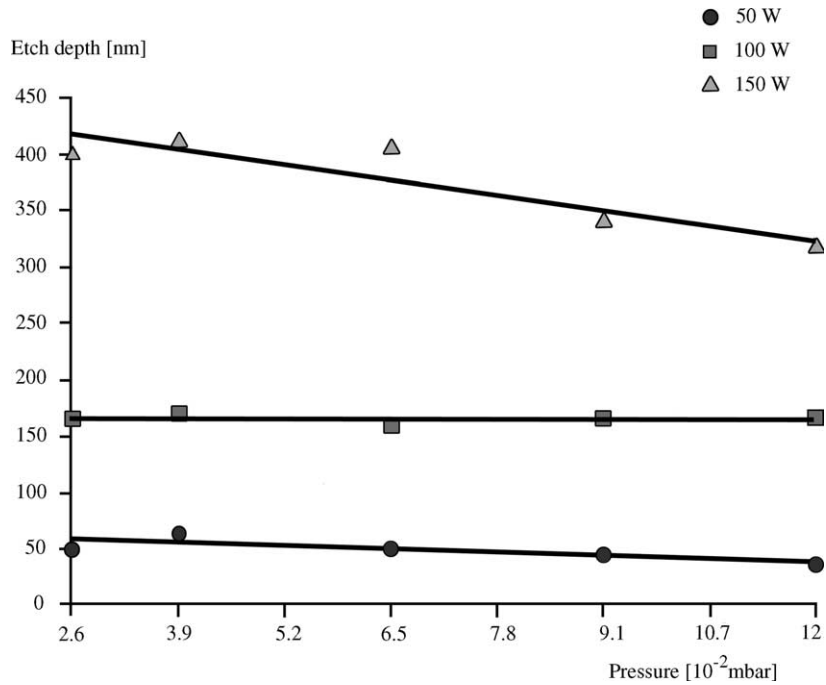


Fig. 4. Variation of etch depth with pressure at different powers.

relative amounts of Ga_2O and Ga_2O_3 . The concentration of Ga_2O was higher at 50 W. This is an important result which will be discussed later in the paper. It is also interesting to note that at

150 W and 10 mT practically the only oxide present on the surface was Ga_2O . As oxides were present, but only at very low concentrations in the argon-treated samples and As_2O_5 disappeared completely

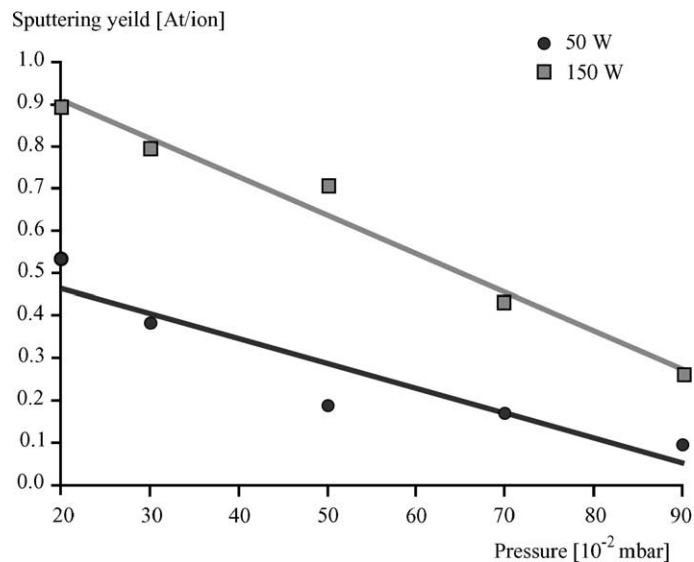


Fig. 5. Variation of experimental sputtering yield with pressure at different powers.

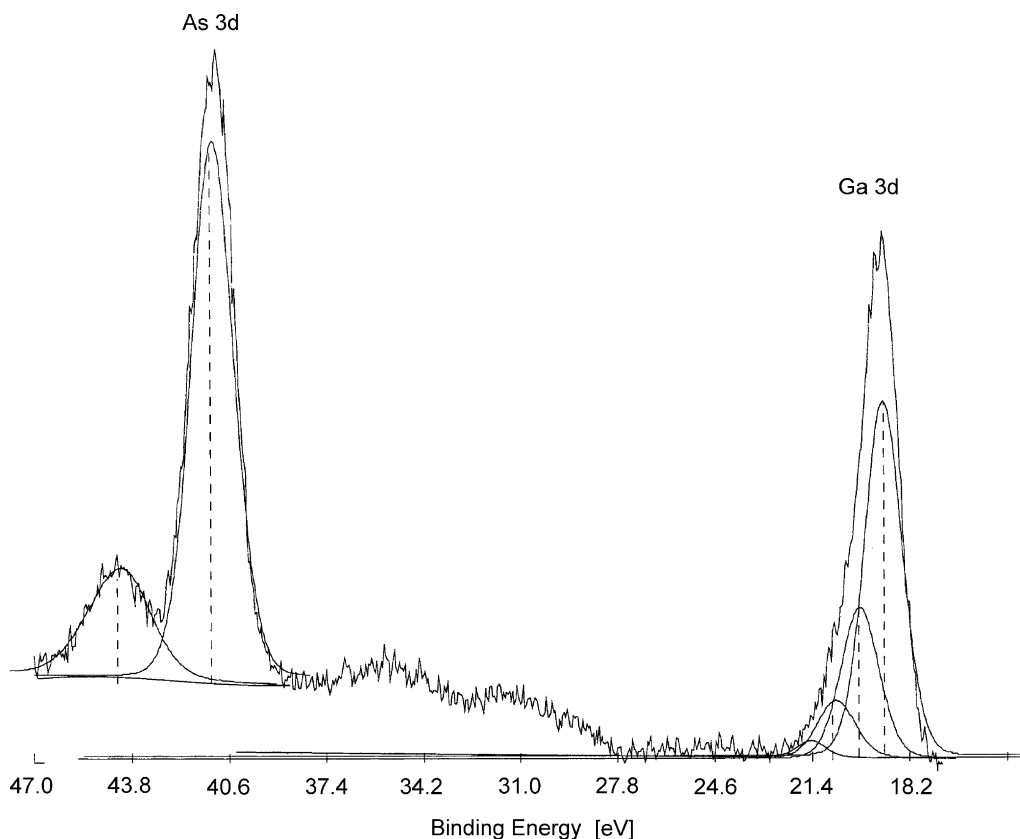


Fig. 6. Typical XPS spectrum of a clean GaAs wafer.

at powers greater than about 50 W. Concentration of $\text{Ga}(\text{OH})_3$ was <5% in all samples.

In the variation of surface composition with power, for powers up to about 50 W the amount of oxide decreased, after this the surface was stable and the predominant oxide was Ga_2O . At 5 W the ion energies are so low that most probably the native oxide was not completely etched. Knowing that some surface oxidation of the sample may occur during transfer in air to the analysis chamber, at least partially, Ga_2O formation may have been due to air exposure. No significant changes of the $(\text{As}/\text{Ga})_s$ ratio were observed with power or pressure.

The variation of the total oxide layer thickness versus pressure and power are shown in Fig. 9(a) and (b). The oxide layer thickness decreased with power to a constant value of between 50 and 100 W at both higher and lower pressures. Below this power range the thickness at 12×10^{-2} mbar was greater than at 1×10^{-2} mbar.

ARXPS analysis for the samples etched at 100 W and 1×10^{-2} mbar and at 12×10^{-2} mbar (see Fig. 10(a) and (b), respectively) showed a fast decrease with depth of the concentration of Ga_2O . The concentration of Ga_2O_3 did not change with depth and a small concentration of As_2O_3 was also observed. At high pressures, the concentration of As_2O_3 increased.

3.2.3. Simulation results using SRIM code

SRIM code [1] can be used to theoretically calculate sputtering yields, number of vacancies, ion ranges, etc. All of the values requested as input for this code are not generally known and they are still controversial. The code provides reasonable values as defaults. For example, the sputtering calculation uses the heat of sublimation to estimate surface binding energy. Although the calculation was performed for a monoenergetic Ar^+ ion beam striking

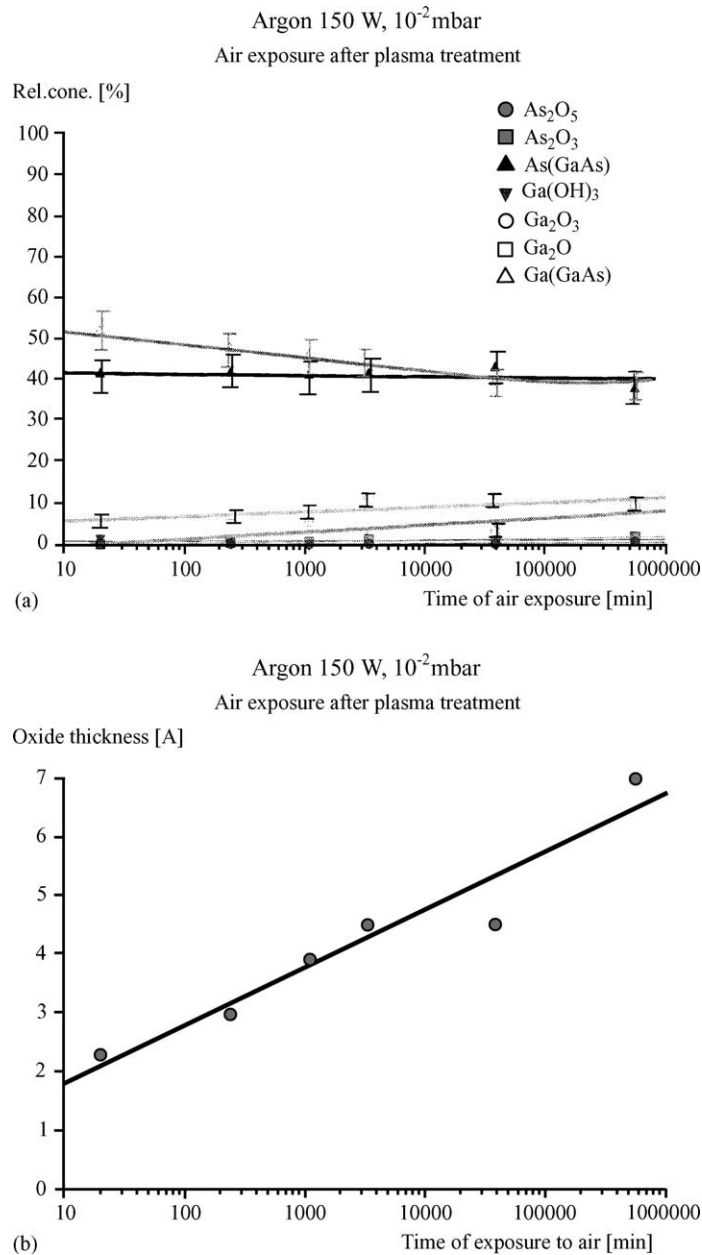


Fig. 7. (a) Surface compositional changes with time for the air-exposed plasma-treated GaAs sample using argon, 150 W, 10^{-2} mbar; (b) oxide layer thickness modification with time.

the surface at normal incidence, some useful information for the case of argon plasma could be obtained.

The penetration depth of ions and of vacancy depth (Fig. 11) increased with ion energy. As can

be observed in this figure, vacancy creation takes place at comparable depths with ion implantation depths for these energies. The calculated total sputtering yield (Y) is given in Fig. 12. Similar results were presented in a comprehensive review of

reported data by Malherbe [19]. According to this author, this code gives overestimated values of sputtering yield especially at low energies (<1 keV). Nevertheless, the important point in a simulation experiment is not to obtain exact values but to determine general trends.

4. Discussion

In order to understand the effects of plasma on the surface, the predominant mechanisms responsible for surface compositional changes have to be identified.

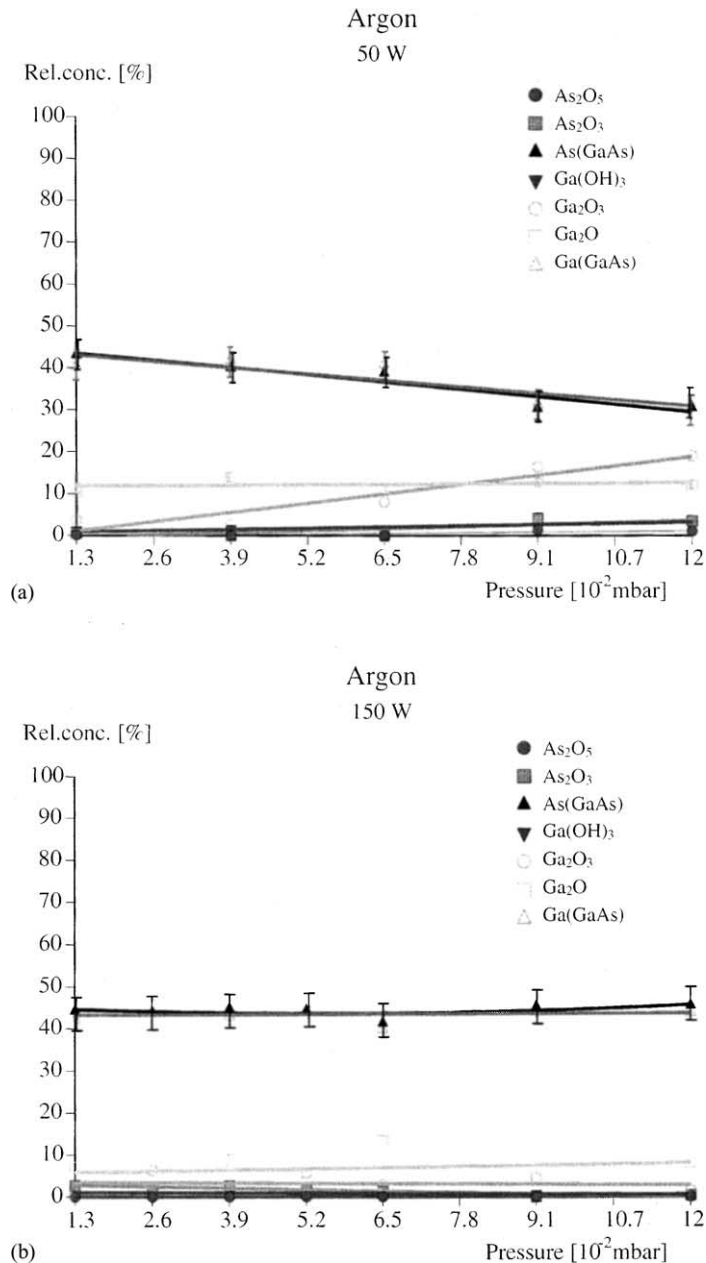


Fig. 8. Variation of surface composition with (a), (b) pressure and (c), (d) power.

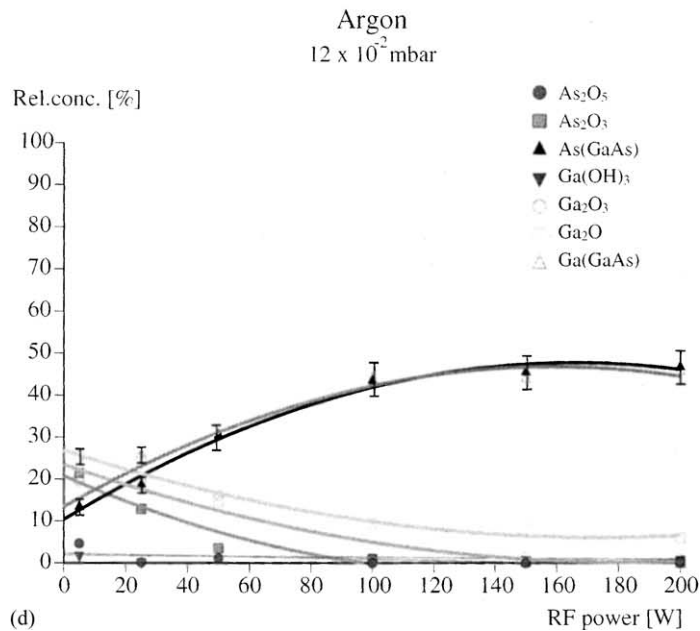
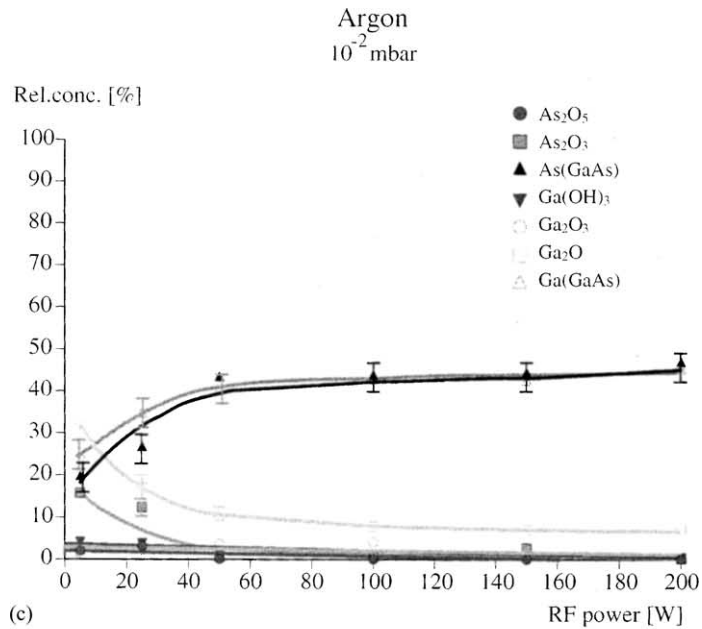


Fig. 8. (Continued).

The sample exposed for a long period of time to the ambient air after plasma treatment was key to the understanding of our results. The data showed that 20 min after extinguishing the plasma the surface did not reach thermodynamic equilibrium. After a month

of exposure to air, the Ga rich GaAs sub-surface became stoichiometric, probably due to surface relaxation and/or the oxidation (Fig. 7(a)). At this stage, it is difficult to separate the processes taking place in the plasma and those occurring in the first

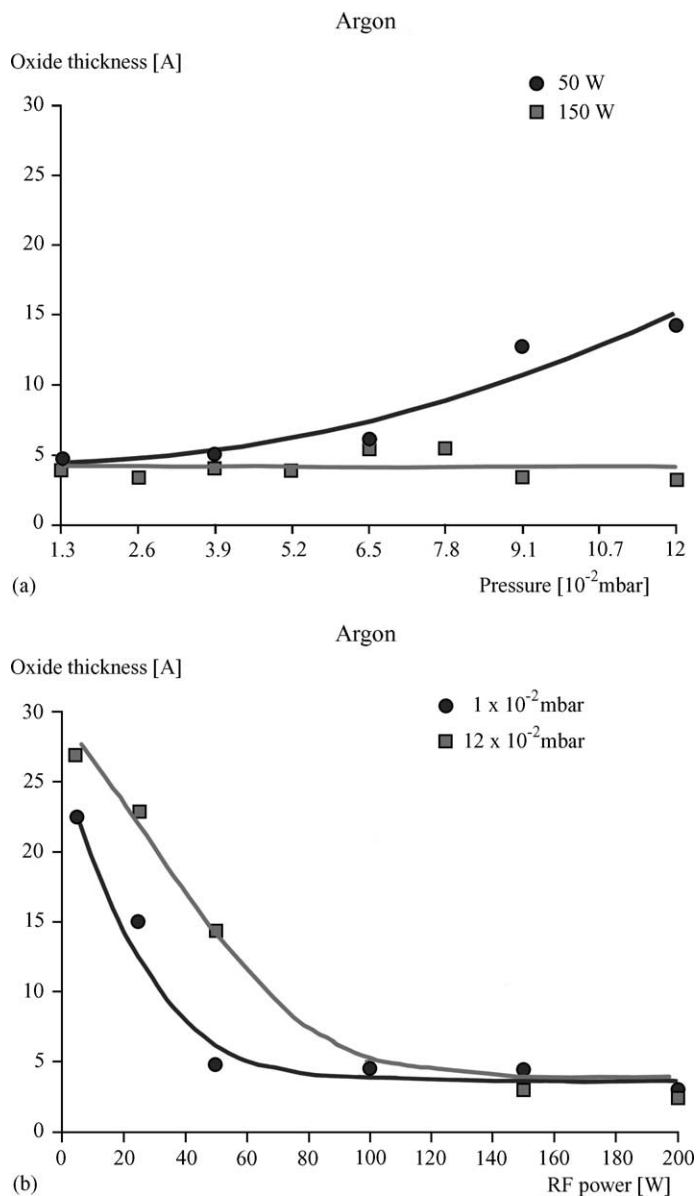


Fig. 9. Variation of oxide layer thickness with (a) pressure and (b) power.

20 min of exposure to air. This is because the typical time interval between etching and XPS analysis for our samples was about 1 month. In this time interval, most of the surface changes had already taken place. This is why no major changes in stoichiometry of the GaAs were found in any of the plasma conditions studied here (Fig. 8(a–d)).

As depletion has been reported in the case of Ar^+ ion bombardment at energies of the order of a few hundreds eV by many authors. Their XPS analyses were undertaken soon after ion bombardment when surface relaxation was far from being completed, and also without air exposure after ion bombardment. As depletion by argon bombardment is also supported by

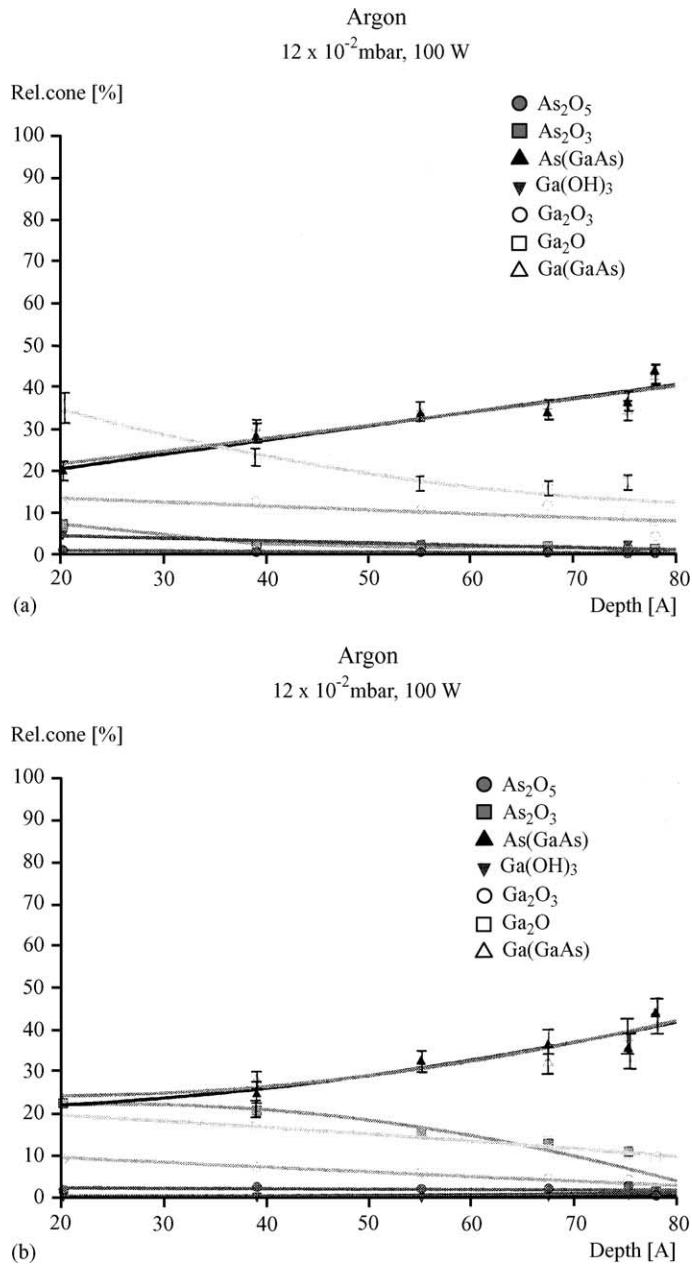


Fig. 10. ARXPS at 100 W and (a) 1×10^{-2} mbar; (b) 12×10^{-2} mbar.

our SRIM results which will be discussed later in this section.

The GaAs surface oxidized in time (Fig. 7(b)) and Ga oxides were mainly formed (Fig. 7(a)). The oxide thickness increased with time logarithmically from about 2.5 to 7 Å over 13 months of exposure to air. It is

impossible to say unequivocally whether the initial oxidation took place during plasma processing or on exposure to air.

Two different plasma conditions will be discussed separately in the following. Their delimitation point will be the value of the power were, at a certain pressure,

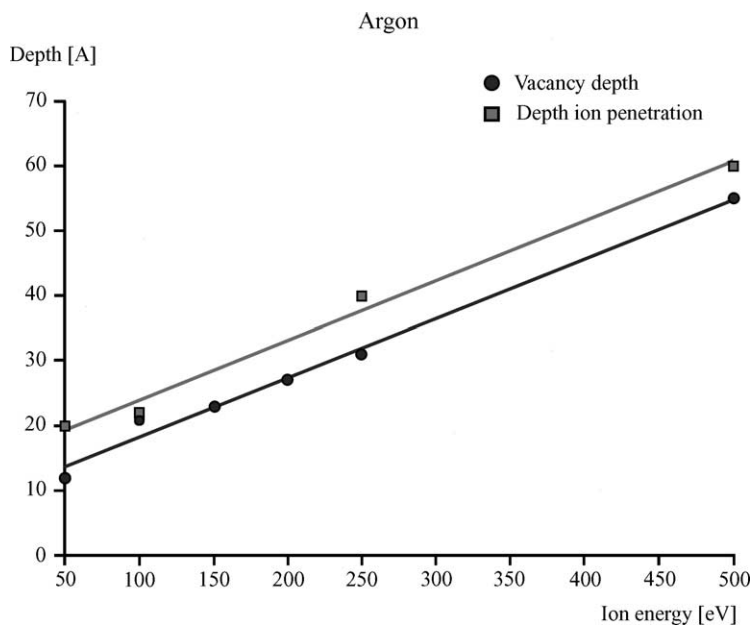


Fig. 11. Calculated penetration depth and vacancy depth (using SRIM).

surface oxidation remained constant with further increase of the power. These two different plasma conditions will be referred to as *weak* and *strong* plasmas. Their delimitation point is different at different pres-

ures. Although surface changes with increasing power were observed only at 10 and 90 mT in this work, there is a strong belief that surface changes at pressures between the two values follow the same trends.

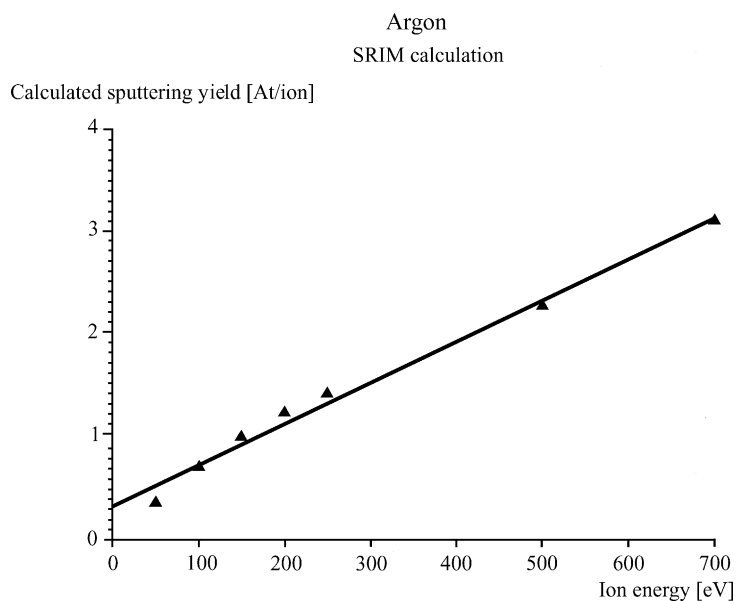


Fig. 12. Calculated sputtering yield (using SRIM).

4.1. Weak plasmas

Because of the fact that the mass of the incident ion is lower than that of surface atoms, for ion energies lower than the binding energy of the surface atom, it is expected [20] that the incident ion is scattered from the surface, transferring only a fraction of its energy to the surface atoms as thermal energy. Also, the surface atom in this collision may be driven towards the bulk. Furthermore, the impurity oxygen present in the plasma may penetrate the surface and create oxides. At these low energies, the native oxide is not removed and the relatively thick oxide layer observed is the sum of these oxides. Another indication for this fact is that even at high energies when the surface is highly activated, only thin oxides (of 5 Å thickness) were formed (Fig. 9(a) and (b)). Thus, the probability is that, when using *weak* plasmas, some oxidation occurs during plasma processing. The fact that only the concentration of Ga₂O₃ changed with pressure and power in the case of *weak* plasmas suggests that its formation has mainly taken place during exposure to plasma. It is known that a virgin GaAs surface consists of a layer of roughly equal amounts of As and Ga oxides [15]. This shows that if no preferential treatment is given to As or Ga (e.g. mechanic polishing of the surface), the surface components oxidize simultaneously. In the case of argon plasma treatment, some preferential treatment must have taken place to account for the differences found in the oxidation and segregation of As and Ga. An important role in surface compositional changes during plasma processing is played by impurities in the plasma. Thus, it is known [17] that hydrogen can form volatile compounds with As. This may be the explanation for the depletion in As oxides observed.

With increasing power, the distribution of ion energies is moved towards higher values and etching becomes more significant than surface oxidation. Similar results have been presented by other authors [2,10,21].

4.2. Strong plasmas

At energies just above the sputtering threshold the surface atoms are directly sputtered by the incoming ions as a result of knock-on collisions. Thus, at higher ion energies (e.g. at least above 50 W at 10 mT and above 150 W at 90 mT), the native oxide was comple-

tely removed. The surface composition did not change with increasing power (Fig. 8(c) and (d)) and the thickness of the oxide layer was constant with increasing power (Fig. 9(b)). The only oxide found on the samples exposed to these plasmas was Ga₂O with a thickness of about 5 Å. Results presented earlier (Fig. 7(a)) showed that on exposure to strong plasmas the stoichiometry of the GaAs surface changed, producing a Ga rich surface layer. This is probably why Ga oxide rich surfaces were observed in the case of *strong* plasmas. Another interesting result is the type of Ga oxide formed at high ion energies, where no oxidation in the plasma has taken place. No explanation for this result can be given at this stage.

The approximately 3 Å increase in the oxide thickness in the time interval between 20 min and a month of air exposure after plasma treatment (see Fig. 7(b)) suggests that at least partially, the surface oxide was formed on the activated surface after the plasma had been extinguished. The rest of the oxide up to the total of 7 Å thickness was either formed in the plasma or in the air immediately after treatment (within the 20 min prior to XPS analysis). We have no means to directly obtain this information, but we believe that this oxide is formed in the air, as well. This is based on the fact that surface oxidation after plasma treatment has a logarithmic growth with time, so most of the oxidation takes place at the beginning of the air exposure, e.g. immediately after the plasma was extinguished. Furthermore, the oxygen in the air has no energy to penetrate the surface, this resulting in the shallow oxidation observed.

XPS cannot give direct information on the composition of the first one or two atomic layers of the surface. XPS signal acquired is an integration of the signal originating from all the layers above the sampling depth. For GaAs, the minimum sampling depth is about 23 Å. As will be seen in the following, SRIM results helped to further understand the phenomena that had taken place during argon plasma treatment of the surface of GaAs.

4.3. SRIM results

Values of the experimentally determined sputtering yield lower than 1 found in all our experiments suggest that not all incoming ions participate to sputtering and collision cascades did not play an important role. Comparison of the experimental sputtering yield with that

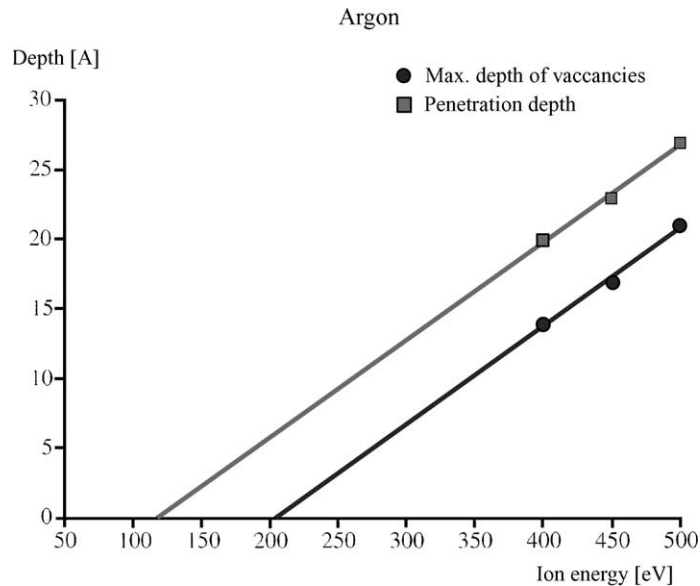


Fig. 13. Penetration depth and vacancy depth adopted for plasma treatment of the surface.

obtained using SRIM showed that a SRIM-estimated sputtering yield below 1 is obtained at energies below 150 eV. Knowing that experimentally determined Y is 1 for ion energies up to about 500 eV, and also that the code gives supra-estimated values, we can consider that the value of 150 eV given by the code is in fact 500 eV. Thus, the replot of Fig. 11 given in Fig. 13 becomes more appropriate for describing the plasma-treated surface processes. The new graph shows that up to about 200 eV, no vacancies are created in the surface and therefore no surface damage is expected at these ion energies. According to Fig. 1, ion energies less than about 200 eV are obtained in *weak* plasmas, at powers lower than about 50 W, all pressures and at powers <150 W at 90 mT. It can also be concluded that As depletion during plasma processing did not take place at least up to this point. These are also the plasma conditions where, using XPS analysis, surface oxidation was found to be more important than sputtering.

At powers above 50 W (*strong* plasmas), creation of vacancies becomes important and for ion energies up to 500 eV the maximum vacancy depth is predicted to be about 20 Å (Fig. 13). Knowing that vacancies provide an easy path for diffusion, segregation of the target atoms towards the surface occurs. The probability of sputtering of an atom raised above the surface is much higher than that of an atom

situated deeper in the surface. Due to the fact that Ga rich surfaces were obtained, we believe that preferential sputtering of As has taken place. The reasons for this are not clear yet. The difference in binding energy between the two constituents of the target may be the explanation for As segregation. For As, this value is 1.26 eV whereas for Ga is 3.075 eV [23].

With increasing ion energy, the predicted increase in vacancy creation may induce further As segregation. The explanation that Ga enrichment of the surface is due, at least partially, to hydrogen contamination is not valid at high ion energies. This is because, as explained earlier, contamination in the plasma (with oxygen and hydrogen compounds) is only important at ion energies below sputtering threshold.

It must be remembered that Fig. 13 refers to ion bombardment and was adapted for plasma processing of the surface. From this figure, it can be observed that surface damage may occur up to about 30 Å depth using ion bombardment at perpendicular incidence to the GaAs surface. In the case of the plasma, the ions have a range of energies; only a fraction of them have the maximum energy and only a small number of these ions strike the surface at normal incidence. Therefore, the maximum depth of damage in the case of plasma may be less than that found for ion bombardment.

5. Conclusions

The above observations allowed us to characterize the surface compositional changes of argon plasma-treated GaAs as follows.

Argon plasma treatment induced important surface oxide growth of tens of angstroms thickness when using *weak* plasmas, at powers <50 W all pressures and also at higher powers and high pressures. These results were explained in terms of reactivity of impurity oxygen in the plasma with the surface. Most of the oxide was formed during plasma processing and consisted of a mixture of Ga and As oxides. The fact that a higher amount of Ga oxide was observed was explained as being due to hydrogen impurities in the plasma which form volatile As compounds.

At powers above 50 W and low pressures (*strong* plasmas), surface etching became more important than oxide formation. The native oxide was first to be removed. Most of the surface oxide found after exposure to *strong* plasmas was formed after plasma treatment and consisted of a thin layer of Ga oxide.

Oxidation during argon plasma treatment and sputtering are two complementary processes, their role depending on the presence of impurities in the plasma and ion energy. Values of about 200 eV for the ion energies were predicted to make the difference between a *strong* and a *weak* plasma.

A very important factor in all experiments is the time elapsed between plasma treatment and surface investigation. This is due to the fact that relaxation processes continue to change the surface composition after exposure to plasma.

Acknowledgements

The authors wish to thank Mr. A. Abbot for technical support and to GEC Marconi for the materials used in this work.

References

- [1] J.F. Ziegler, J.P. Biersack, U. Littmark, *The Stopping and Range of Ions in Solids*, 2nd ed., New York, Pergamon, 1985.
- [2] D. Kuen-Sane, H. Rong-Yih, *Materials science and engineering B—solid state materials for advanced technology B* 9 (1-3) (1991) 57.
- [3] I.L. Singer, J.S. Murday, J. Comas, *J. Vac. Sci. Technol.* 18 (2) (1981) 161.
- [4] J.B. Malherbe, W.O. Barnard, I. Strydom, C.W. Louw, *Surf. Interf. Anal.* 18 (1992) 491.
- [5] A. Scandurra, A. Licciardello, A. Torrisi, *Appl. Surf. Sci.* 103 (1996) 19.
- [6] J.L. Sullivan, W. Yu, S.O. Saied, *Appl. Surf. Sci.* 90 (1995) 309.
- [7] T. Aoyama, M. Tanemura, F. Okuyama, *Appl. Surf. Sci.* 100/101 (1995) 351–354.
- [8] J.T. Wolan, C.K. Mont, G.B. Hoflund, *Appl. Phys. Lett.* 72 (1998) 1469.
- [9] C. Ching-Hui, D.L. Green, E.L. Hu, *J. Vac. Sci. Technol. B* 13 (6) (1995) 2355.
- [10] J.S. Pan, A.T.S. Wee, C.H.A. Huan, H.S. Tan, K.L. Tan, *J. of Phys. D: Appl. Phys.* 30 (1997) 2514.
- [11] Y. Wei, *Ion Bombardment Induced Compositional Changes in Compound Semiconductor Surfaces Studied by XPS Combined with LEISS*, Ph.D., Aston University, UK, 1995.
- [12] S. Rauf, M.J. Kushner, *J. Appl. Phys.* 82 (6) (1997) 2805.
- [13] V.A. Godyak, R.B. Piejak, N. Sternberg, *IEEE Trans. Plasma Sci.* 21 (4) (1993) 378.
- [14] C. Lai, R.A. Breun, P.W. Sandstrom, A.E. Wendt, N. Hershkovitz, R.C. Woods, *J. Vac. Sci. Technol. A* 11 (4) (1993) 1199.
- [15] C.C. Surdu-Bob, S.O. Saied, J.L. Sullivan, *Appl. Surf. Sci.* 183 (2001) 126.
- [16] D. Briggs, M.P. Seah, *Practical Surf. Analysis*, 2nd ed., Wiley, Chichester, 1990.
- [17] R.L. Layberry, *Computer Simulation of Radio-Frequency Methane/Hydrogen Plasmas and their Interaction with GaAs Surfaces*, Ph.D., Aston University, UK, 1999.
- [18] M.J. Chester, T. Jach, *J. Vac. Sci. Technol. B* 11 (4) (1993) 1609–1613.
- [19] J.B. Malherbe, *Sputtering of compound semiconductor surfaces. Part 1. Ion-solid interaction and sputtering yields*, *Critical Rev. Solid State Mater. Sci.* 19 (2) (1994) 55–127.
- [20] M. Kaminsky, Washington, DC, American Chemical Society, 1976.
- [21] T. Choudhury, Ph.D., Aston University, UK, 1991.
- [22] I.A. Russu, Ph.D. A.I. Cuza University, Romania, 2001.
- [23] J.S. Pan, A.T.S. Wee, C.H.A. Huan, H.S. Tan, K.L. Tan, *J. Phys. D: Appl. Phys.* 30 (1997) 2514–2519.